# Orientation-Dependent Final-State Effects in Photoelectron Spectra of Physisorbed Molecules

A. Nilsson,(1) R. E. Palmer,(2) H. Tillborg,(1) B. Hernnäs,(1) R. J. Guest,(2) and N. Mårtensson(1)
(1)*Department of Physics, Uppsala University, Box 530, S-751 21 Uppsala, Sweden*
(2)*Cavendish Laboratory, Madingley Road, Cambridge, CB3 0HE, United Kingdom*

(Received 18 October 1991)

We report high-resolution core- and valence-level photoemission and core-to-valence x-ray-absorption spectra of $O_2$ physisorbed on graphite. The submonolayer $\delta$-$\zeta2$ orientational phase transition is manifest in the core-level spectrum as an extra broadening of each component of the paramagnetically split O 1$s$ doublet. This phase transition is not visible in the $1\Pi_g$ valence spectrum or the $1s \rightarrow 1\Pi_g$ absorption line. The results reflect the detailed shape of the charge distribution in the final state of the molecule. We suggest that the population of low-frequency librational modes makes an important contribution to the core-level linewidths.

PACS numbers: 68.35.Rh, 68.35.Bs, 68.35.Ja, 79.60.Gs

The role of final-state effects in photoemission from adsorbed molecules is a subject of considerable interest [1-3]. It has now been convincingly established that the shifts in binding energy, relative to the gas phase, of both the core and valence levels observed in photoemission studies of atoms and molecules weakly bound to metallic surfaces contain important contributions from final-state effects, in particular, from image screening of the positively charged ion produced by emission of the photoelectron [4]. Similarly, this screening contributes to the shifts in energy of the molecular negative-ion states observed as resonances in electron energy-loss spectroscopy studies [5,6] of physisorbed molecules on metallic surfaces. For a given ionic state in an adsorbed atom [4] or adsorbed molecule of fixed orientation [7], the shift in energy of the positive or negative ion as a function of distance from the metal is accurately modeled by treating the ion as a point charge in a classical image potential. In this Letter we present experimental results which show, however, that the precise spatial distribution of the charge in different ionic states of a given molecule, together with the orientation of the molecule, determines the manner in which these states couple to the metallic screening potential. We exploit these effects to demonstrate how core-level x-ray photoelectron spectroscopy (XPS) can be used to locate an orientational phase transition (even) in a physisorbed molecular monolayer. We investigate in a systematic fashion the energy shifts and line-shape perturbations of the core (1$s$) and valence ($1\Pi_g$) levels in photoemission from $O_2$ physisorbed on graphite, as well as the x-ray-absorption ($1s \rightarrow 1\Pi_g$) spectrum. In the case of the core-ionized molecule, the positive charge distribution of the final state is asymmetric (due to the localization of the core hole), so that the submonolayer phase transition [8,9] in the $O_2$/graphite system from the low-coverage $\delta$ phase (molecules lying down) to the higher-coverage $\zeta2$ phase (standing up) manifests itself in the O 1$s$ line shape. The $\delta$-$\zeta2$ phase transition is invisible in the valence-ionized spectrum (symmetric positive charge distribution) and the x-ray-absorption line (neutral final state). The asymmetry of the positive final state in the core-level spectrum is also found to lead to a significant extra broadening of the spectral lines in all surface phases.

The photoelectron spectrometer has been described previously [10]. The overall instrumental resolution was 0.25 eV for XPS and 0.1 eV for ultraviolet photoemission spectroscopy (UPS). The x-ray absorption (XAS) spectra were recorded at MAX-Lab with an overall resolution of 0.3 eV [11]. All measurements were performed at 25 K.

Figure 1 shows the x-ray photoemission spectrum of

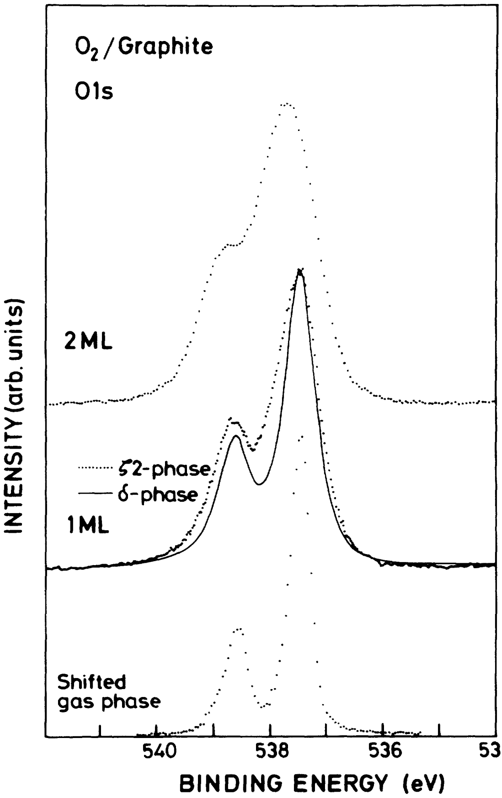

FIG. 1. O 1$s$ x-ray photoemission spectrum of molecular $O_2$ physisorbed on graphite in the monolayer $\delta$ and $\zeta2$ phases and the bilayer. The corresponding gas-phase spectrum (Ref. [12]) is shown for comparison.

the O 1$s$ core level obtained at three different coverages of $O_2$ on (highly oriented pyrolitic) graphite, corresponding to the saturated submonolayer $\delta$ phase, the monolayer $\zeta 2$ phase, and the bilayer. The (shifted) gas-phase spectrum [12] (instrumental resolution 0.3 eV) is also reproduced for comparison. In general terms, one is struck by the broad similarity between the surface and gas-phase spectra. In particular, the paramagnetic splitting of the core line in the gas phase, arising from two final states with different spins ($^4\Sigma$ and $^2\Sigma$), is preserved on the surface, even in the $\delta$ phase where antiferromagnetic ordering of the magnetic moments of the paramagnetic $O_2$ molecules has been predicted [13]. The value of the paramagnetic splitting in the XPS spectrum, 1.2 eV, may be compared with the larger paramagnetic splitting, 3 eV, proposed by Wurth *et al.* [14] in their interpretation of the near-edge x-ray-absorption fine structure (NEXAFS) spectrum of physisorbed $O_2$ on Pt(111). Regarding the details of the spectra in Fig. 1, three key points can be made: (i) There is a binding-energy shift, with respect to the gas phase, of (both components of) the 1$s$ line in each of the surface phases, 1.5 eV in the $\delta$ and $\zeta$ phases, and 1.2 eV in the bilayer phase (the binding energy, with respect to the Fermi level, of the stronger component of the doublet is 537.4 eV in the $\delta$ and $\zeta$ phases, 537.7 eV in the bilayer, and 538.9 eV in the gas phase, assuming the graphite work function is 4.5 eV). (ii) The width of each component of the doublet is substantially increased in each of the surface phases compared with the gas phase (where the measured width is 0.41 eV [15]). (iii) The measured width [full width at half maximum (FWHM)] of each of the lines in the $\zeta 2$ phase (1.05 eV) is significantly larger than that in the $\delta$ phase (0.75 eV), i.e., the $\delta$-$\zeta 2$ orientational phase transition manifests itself in the core-level spectrum. The binding-energy shift between the monolayer and the bilayer is used to define monolayer (i.e., $\zeta 2$ phase) completion [4]; the coverage needed to prepare the saturated $\delta$ phase is then derived from the relative densities of these phases [16], and confirmed by NEXAFS [17]. We shall return to a discussion of the detailed shifts and broadenings of the 1$s$ lines after a description of the spectral lines seen in x-ray-absorption spectroscopy and ultraviolet photoemission spectroscopy.

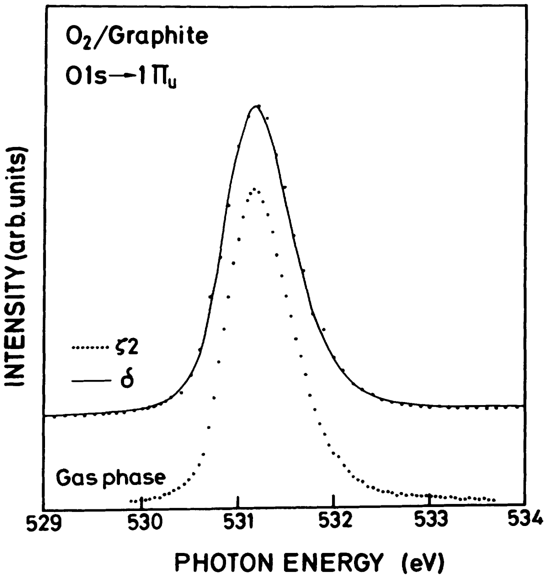

FIG. 2. X-ray-absorption spectrum of $O_2$ physisorbed on graphite in the $\delta$ and $\zeta 2$ phases showing the O $1s \rightarrow 1\Pi_g$ absorption line. The corresponding gas-phase spectrum (Ref. [18]) is shown for comparison.

Figure 2 shows the x-ray-absorption line corresponding to the core-to-valence, $1s \rightarrow 1\Pi_g$, intramolecular electronic excitation. Data for both the $\delta$ phase and the $\zeta 2$ phase are shown, together with the (shifted) gas-phase spectrum [18] for comparison. The peak in the absorption line in each phase is shifted by 0.3 eV in energy with respect to the gas phase, a modest shift which can be attributed to the lack of a precise calibration in the gas-phase work [19]. The absence of any large shift, compared with those seen in the XPS spectra, exposes the role played by the final state in the excitation process; image potential screening (by the substrate) and polarization screening (by the coadsorbed $O_2$ molecules) substantially shift the energy of the positively ionized final state in XPS compared with the neutral final state in XAS. Of particular significance in Fig. 2 is that the absorption line looks virtually identical in the $\delta$ and $\zeta 2$ phases (and is very similar to that seen in the gas-phase spectrum), i.e., the $\delta$-$\zeta 2$ orientational phase transition is not manifest in the x-ray-absorption spectrum. The measured linewidth (FWHM) of 0.87 eV in both phases on the surface compared with 0.84 eV in the gas is attributable to the higher resolution in the gas-phase spectrum and represents a very small perturbation upon adsorption [20].

In Fig. 3 we present the UPS spectra of the $1\Pi_g$ valence level of $O_2$ in the $\delta$, $\zeta 2$, and bilayer phases on graphite, and also show the corresponding gas-phase spectrum [21] (shifted by 1.3 eV). The gas-phase data show the well-established vibrational fine structure arising from the population of vibrational levels of the positively ionized $^2\Pi_g$ final state in the photoemission process [22]. Figure 3 demonstrates that this fine structure is preserved in the physisorbed phases, though the individual peaks in the fine structure are broadened, and the distribution of intensity among these peaks is different [22]. The valence-level spectra of the $\delta$ and $\zeta 2$ phases are virtually identical, i.e., the $\delta$-$\zeta 2$ phase transition is not manifest in the valence-level photoemission spectrum. The measured width (FWHM) of the vibrational peaks is approximately 0.25 eV in both the $\delta$ and $\zeta 2$ phases, compared with the much sharper lines in the gas phase.

The increase in the width of the $^2\Pi_g$ vibronic peaks in the $O_2$ monolayer phases over the gas phase compares with the negligible change in the width of the $1s \rightarrow 1\Pi_g$ XAS line upon adsorption, and with the larger broaden-

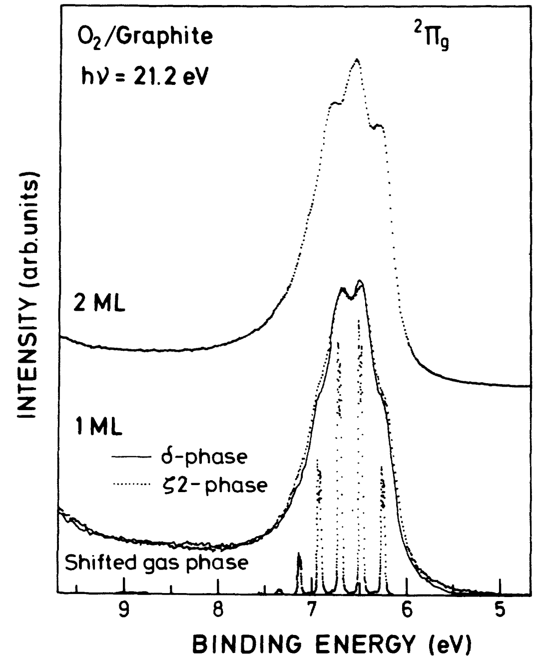

FIG. 3. Ultraviolet photoemission spectrum of $O_2$ physisorbed on graphite in the $\delta$ and $\zeta 2$ phases and in the bilayer. The corresponding gas-phase spectrum (Ref. [21]) is shown for comparison.

ing, by about 0.5 and 1 eV, respectively, of the 1*s* XPS line in the $\delta$ and $\zeta 2$ phases over that in the gas phase. The line shape in these various spectroscopies is therefore seen to be highly sensitive to the final state produced by excitation or removal of the electron. This observation forms a starting point in addressing the question of why the $\delta$-$\zeta 2$ phase transition is evident in the core-level photoemission spectrum but not in the valence-level photoemission spectrum or in the core-to-valence absorption spectrum. It also allows us to account for the substantial extra broadening of the O 1*s* XPS line in the physisorbed phases compared with the gas phase.

We propose that the key reason why the $\delta$-$\zeta 2$ orientational phase transition of the $O_2$ monolayer is seen only in the core-level XPS spectrum is that in this case the final state is positively charged and, because of the localization of the core hole on one or other of the oxygen atoms in the molecule, asymmetric [23]. By contrast, the final state in the XAS spectrum is neutral, while in the UPS case, though the final state is positively charged, the delocalization of the valence hole means that the charge distribution is highly symmetric with respect to inversion through the center of the molecule. The positively charged final state leads to strong image potential (and polarization) screening of the final state in the core-level spectrum; the asymmetry of the charge distribution means that this screening is sensitive to the orientation of the molecule on the surface. Thus, in the $\delta$ phase the $O_2$ molecules are lying down and core holes localized on either of the two oxygen atoms in an $O_2$ molecule are equivalent. By contrast, in the $\zeta 2$ phase the $O_2$ molecules are standing up and the core hole localized on the oxygen atom further from the surface is screened in a different fashion from the core hole on the other oxygen atom. In particular, the degree of screening by the metallic image potential will be a function of distance from the surface. One can thus envisage that the broad lines in the core-level spectrum of the $\zeta 2$ phase arise from the superposition of two core-level spectra reflecting the different core-hole locations. The delocalization of the final-state positive charge in the valence-level spectrum quenches the sensitivity of the UPS line shape to the orientation of the molecule, while the neutral final state in the absorption spectrum means that screening of the final state is weak whatever the orientation of the molecule.

To address the question of why the core-level spectrum is more substantially broadened in comparison with the gas phase, in all surface phases, than the valence or absorption spectrum, we have to consider the detailed mechanism by which the proposed image screening operates. A number of mechanisms have been suggested to account for the universal broadening observed in the photoemission lines of adsorbed species [24]. In physisorbed species the range of possibilities is narrowed because there is no bonding overlap with the substrate. It has been shown that lifetime broadening makes only a small contribution to the widths in physisorbed molecules [2,25]. The excitation of electron-hole-pair excitations in the metallic substrate can also be discounted as the major cause of the broadening of the O 1*s* line (Fig. 1) because the width of the C 1*s* line in graphite itself [26], where one would expect the contribution of electron-hole pairs to be manifest, is only 0.28 eV [27]. Further, electron-hole-pair broadening should be evident in the $1\Pi_g$ valence line (Fig. 2) as well as in the O 1*s* line, so does not account for the larger width of the core lines. Other mechanisms proposed to account for the widths of valence-band features [1,2] would broaden the oxygen valence level rather than the core level.

One further mechanism advanced to account for line broadening in adsorbed atoms and molecules is the population of closely spaced (unresolved) vibronic bands in the final state [3,28]. These closely spaced vibrational levels represent the new low-frequency frustrated translational and rotational modes which arise when a molecule is bound to a surface and surrounded by neighboring molecules, and the population of these states is analogous to the population of the intramolecular vibrational modes in the UPS $1\Pi_g$ spectrum (Fig. 2). In quantum mechanical terms, this mechanism corresponds to the excitation of quantized vibrational motion in the final state. Classically, the broadening can be understood as an averaging of the image potential and polarization screening of the ionized final state as the ionized atom or molecule slowly vibrates. Because this mechanism depends on the local details of the potential energy surface on which the atoms in question vibrate, it can in principle explain the substantial broadening of the O 1*s* level in the absence of a similar broadening in the C 1*s* level of the graphite substrate or in the Ar 2*p* core level. If we suppose that the large-amplitude low-frequency modes needed for this mechanism are hindered rotational (i.e., librational) modes rather than hindered translational (i.e., vibrational) modes, this mechanism can also account for the more substantial broadening of the XPS spectrum compared with the UPS spectrum. In the screening-average picture, the energy of the molecular ion with a symmetric charge distribution (UPS final state) does not change much as the molecule slowly librates on the surface, whereas the energy of the ion with an asymmetric charge distribution (XPS final state) is more sensitive to the orientation of the molecule. Mean-field calculations [29] of the librational motion in the $\delta$ phase of $O_2$ on graphite indicate two librational modes, one parallel to the surface (with frequency 4.5 meV) and one perpendicular to the surface (7.5 meV), with root-mean-square amplitudes of the order of 10° in each case at 20 K. Resonance electron energy-loss spectroscopy [8] and near-edge x-ray-absorption fine structure measurements [16] indicate possibly larger tilts of around 20° in both the $\delta$ and $\zeta 2$ phases. These modes are the contenders for the librational-mode broadening mechanism which we suggest may account for the observed results. Clearly, detailed theoretical modeling of this new effect would be very desirable [30].

We thank Dr. A. W. Moore, Union Carbide, for supplying the pyrolitic graphite samples and the staff of MAX-Lab for their assistance. We are grateful for financial support by the Swedish Natural Science Research Council, the Swedish Board for Technical Development, the Bank of Sweden Tercentenary Foundation, the Royal Society, and ICI plc. R.J.G. thanks the United Kingdom SERC for support via a studentship.

---

[1] M. Bertolo, W. Hansen, and K. Jacobi, Phys. Rev. Lett. **67**, 1898 (1991).
[2] U. Höfer, M. J. Breitschafter, and E. Umbach, Phys. Rev. Lett. **64**, 3050 (1990); U. Höfer and E. Umbach, J. Electron Spectrosc. Relat. Phenom. **54/55**, 591 (1990).
[3] A. Nilsson and N. Mårtensson, Phys. Rev. Lett. **63**, 1483 (1989); Solid State Commun. **70**, 923 (1989).
[4] T. Mandel, G. Kaindl, M. Domke, W. Fischer, and W. D. Schneider, Phys. Rev. Lett. **55**, 1638 (1985); T.-C. Chiang, G. Kaindl, and T. Mandel, Phys. Rev. B **33**, 695 (1986).
[5] P. J. Rous, E. T. Jensen, and R. E. Palmer, Phys. Rev. Lett. **63**, 2496 (1989).
[6] R. E. Palmer and P. J. Rous, Rev. Mod. Phys. (to be published); L. Sanche, J. Phys. B **23**, 1597 (1990).
[7] A. Gerber and A. Herzenberg, Phys. Rev. B **31**, 6219 (1985); D. Teillet-Billy and J. P. Gauyacq, Nucl. Instrum. Methods Phys. Res., Sect. B **58**, 393 (1991); P. J. Rous, Surf. Sci. (to be published).
[8] E. T. Jensen, R. E. Palmer, and P. J. Rous, Phys. Rev. Lett. **64**, 1301 (1990); Surf. Sci. **237**, 153 (1990).
[9] M. F. Toney and S. C. Fain, Jr., Phys. Rev. B **36**, 1248 (1987).
[10] A. Nilsson and N. Mårtensson, Phys. Rev. B **40**, 10249 (1989).
[11] J. N. Anderssen, O. Björneholm, A. Sandell, R. Nyholm, J. Forsell, L. Thanell, A. Nilsson, and N. Mårtensson, Synchrotron Radiat. News **4**, 21 (1991).
[12] M. Larsson, P. Baltzer, S. Svensson, B. Wannberg, N. Mårtensson, A. Naves de Brito, N. Correia, M. P. Keane, M. Carlsson-Göthe, and L. Karlsson, J. Phys. B **23**, 1175 (1990).
[13] R. D. Etters and O. B. M. Hardouin Duparc, Phys. Rev. B **32**, 7600 (1985).
[14] W. Wurth, J. Stöhr, P. Feulner, X. Pan, K. R. Bauchspeiss, Y. Baba, E. Hudel, G. Rocker, and D. Menzel, Phys. Rev. Lett. **65**, 2426 (1990).
[15] The more intense ($^4\Sigma$) component of the doublet in the gas phase is dominated by a single vibrational state.
[16] H. You and S. C. Fain, Jr., Phys. Rev. B **33**, 5886 (1986).
[17] R. J. Guest, A. Nilsson, O. Björneholm, B. Hernnäs, A. Sandell, R. E. Palmer, and N. Mårtensson, Surf. Sci. (to be published).
[18] M. Domke, T. Mandel, A. Puschmann, S. Xve, D. Shirley, G. Kaindl, H. Petersen, and P. Koski, Rev. Sci. Instrum. (to be published).
[19] We calibrate the photon energy by measuring the difference in the kinetic energy of electrons photoemitted by first- and second-order light.
[20] The large width of the gas-phase line is due to the population of a broad distribution of vibrationally excited states.
[21] P. Baltzer, L. Karlsson, and B. Wannberg (to be published).
[22] W. Eberhardt and E. W. Plummer, Phys. Rev. Lett. **47**, 1476 (1981).
[23] D. Nordfors, H. Ågren, and K. V. Mikkelson (to be published).
[24] N. Mårtensson and A. Nilsson, J. Electron Spectrosc. Relat. Phenom. **52**, 1 (1990).
[25] M. Coville and T. D. Thomas, Phys. Rev. A **43**, 6053 (1991), have shown that the lifetime broadening of the O 1*s* level (around 0.15 eV) is not very sensitive to the chemical environment.
[26] F. Sette, G. K. Wertheim, Y. Ma, G. Meigs, S. Modesti, and C. T. Chen, Phys. Rev. B **41**, 9766 (1990).
[27] In the case of the 2*p* core level in Ar physisorbed on graphite, where electron-hole-pair broadening should also be seen, we find a width of 0.35 eV, much less than that of the O 1*s* line.
[28] J. W. Gadzuk, S. Holloway, C. Mariani, and K. Horn, Phys. Rev. Lett. **48**, 1288 (1982).
[29] R. D. Etters and K. Kobashi, J. Chem. Phys. **81**, 6249 (1984).
[30] Recent theoretical modeling (Ref. [23]) in the case of a *single* molecule interacting with the substrate can only partly explain the effect.